Articles

A Theoretical Study of Homogeneous Ziegler−Natta Catalysis

Fernando Bernardi, Andrea Bottoni,* and Gian Pietro Miscione

Dipartimento di Chimica "G. Ciamician", Universitá di Bologna, via Selmi 2, 40126 Bologna, Italy

Received February 28, 1997[⊗]

In this paper we have investigated, using a DFT (B3LYP) computational approach, the insertion process of ethylene in the titanium−carbon bond, which represents a fundamental step in the Ziegler−Natta polymerization reaction. The DFT results have been validated by a comparison with the results obtained at the MP2 and CASPT2 levels. The two following models have been considered: (i) the cationic species $Cl_2TiCH_3^+$ reacting with an ethylene molecule which emulates the positive part of a solvent-separated ion pair $(CH_3)_2AlCl_2^-$ || $Cl_2TiCH_3^+$); (ii) the bimetallic species $H_2Al(\mu\text{-}Cl)_2TiCl_2CH_3$ also reacting with ethylene and which mimics the possible bimetallic complexes or tight ion pairs that can originate from the catalyst−cocatalyst interaction. In the former case the process is highly exothermic (−45.5 kcal mol^{-1}) and is characterized by an insertion energy barrier of about 5 kcal mol^{-1}. In the latter case the energetically most favored channel is a two-step reaction path that requires the overcoming of a first barrier of about 5.6 kcal mol^{-1} to form an intermediate and of a second barrier of 5.8 kcal mol^{-1} to reach the insertion transition state. We suggest that in the real conditions used to carry out the reactions both reaction channels (bimetallic complex and separated ion pair) are simultaneously available and that their relative importance and the resulting reaction rate are determined by the solvent polarity: the more polar the solvent, the more important the reaction path involving the cationic species. Self-consistent isodensity polarized continuum model (SCI-PCM) computations have shown that the insertion barriers decrease with the increasing polarity of the solvent.

Introduction

The Ziegler−Natta polymerization of olefins represents an important industrial process which is capable of polymerizing olefins in long molecular chains. It is extremely fast and can proceed with high stereoselectivity. Because of its relevance, a great deal of experimental[1,2] and theoretical[3] work has been carried out on this reaction, and several mechanistic schemes have been suggested.

The commonly accepted mechanism for Ziegler−Natta catalysis is that proposed by Cossee.[1k,l] According to this mechanism (see Scheme 1) the catalyst in its active form is characterized by a vacant site which binds an olefin to form a metal−alkyl−olefin complex (step 1). In a subsequent step (step 2) the olefin inserts into the metal−alkyl bond through a four-center transition state. This step leads to a new alkyl complex characterized by a longer chain (growing chain) and by a new vacant site on the metal which can bind another olefin mol-

[⊗] Abstract published in *Advance ACS Abstracts*, December 1, 1997.

(1) (a) Breslow, D. S.; Newburg, N. R. *J. Am. Chem. Soc.* **1957**, *79*, 5072. (b) Natta, G.; Pino, P.; Giannini, V.; Mantica, E.; Peraldo, M. *J. Polym. Sci.* **1957**, *26*, 120. (c) Breslow, D. S.; Newburg, N. R. *J. Am. Chem. Soc.* **1959**, *81*, 81. (d) Chien, J. C. W. *J. Am. Chem. Soc.* **1959**, *81*, 86. (e) Duck, E. W. *J. Polym. Sci.* **1959**, *34*, 49. (f) Natta, G.; Pasquon I. *Adv. Catal.* **1959**, *11* , 1. (g) Long, W. P. *J. Am. Chem. Soc.* **1959**, *81*, 5312. (h) Bestian, H.; Clauss, K. *Angew. Chem., Int. Ed. Engl.* **1963**, *2*, 704. (i) Cossee, P. *J. Catal.* **1964**, *3*, 65. (j) Arlman, E. J.; Cossee, P. *J. Catal.* **1964**, *3*, 80, 89, 99. (k) Cossee, P. *Recl. Trav. Chim. Pays-Bays* **1966**, *85*, 1151. (l) Henrici-Olive', G.; Olive', S. *Angew. Chem., Int. Ed. Engl.* **1971**, *10*, 105. (m) Cassoux, P.; Crasnier, F.; Labarre, J. F. *J. Organomet. Chem.* **1971**, *165*, 303. (n) Armstrong, P. R.; Perkins, P. G.; Stewart, J. J. P. *J. Chem. Soc., Dalton Trans.* **1972**, 1972. (o) Machon, J.; Hermant, R.; Houteaux, J. P. *J. Polym. Sci. Symp.* **1975**, *52*, 107. (p) Fink, G.; Rottler, R.; Schnell, D.; Zoller, W. *J. Appl. Polym. Sci.* **1976**, *20*, 2779. (q) Chien, J. C. W. *J. Polym. Sci. Part A: Polym. Chem.* **1988**, *26*, 2369. (r) Chien, J. C. W.; Sugimoto, R. *J. Polym. Sci. Part A: Polym. Chem.* **1991**, *29*, 459. (s) Chien, J. C. W.; Rausch M. D.; Tsai, W. *J. Am. Chem. Soc.* **1991**, *113*, 8570.

(2) (a) Eisch, J. J.; Piotrowsky, A. M.; Brownstein, S. K.; Gabe, E. J.; Lee, F. L. *J. Am. Chem. Soc.* **1985**, *107*, 7219. (b) Fink, G.; Zoller, W. *Makromol. Chem.* **1981**, *182*, 3265. (c) Yang, X.; Stern, C.; Marks, J. J. *J. Am. Chem. Soc.* **1991**, *113*, 3623. (d) Eisch, J. J.; Caldwell, K. W.; Werner, S.; Krueger, C. *Organometallics* **1991**, *10*, 3417. (e) Eisch, J. J.; Pombrik, S. I.; Zheng, G. *Organometallics* **1993**, *12*, 3856.

(3) (a) Novaro, O.; Blaisten-Barojas, E.; Clementi, E.; Giunchi, G.; Ruiz-Vizcaya, M. E. *J. Chem. Phys.* **1978**, *68*, 2337. (b) Fujimoto, H.; Yamasaki, T.; Mizutani, H.; Koga, N. *J. Am. Chem. Soc.* **1992**, *107*, 6157. (c) Kawamura-Kuribayashi, H.; Koga, N.; Morokuma, K. *J. Am. Chem. Soc.* **1992**, *114*, 2359. (d) Axe, F. U.; Coffin, J. M. *J. Phys. Chem.* **1994**, *98*, 2567. (e) Meier, R. J.; van Doremaele, G. H. J.; Iarlori, S.; Buda, F. *J. Am. Chem. Soc.* **1994**, *116*, 7274. (f) Woo, J. K.; Fan, L.; Ziegler, T. *Organometallics* **1994**, *13*, 2252. (g) Weiss, H.; Ehrig, M.; Ahlrichs, R. *J. Am. Chem. Soc.* **1994**, *116*, 4919. (h) Jensen, V. R.; Børve, K. J.; Ystenes, M. *J. Am. Chem. Soc.* **1995**, *117*, 4109. (i) Lohrenz, J. C. W.; Woo, T. K.; Ziegler, T. *J. Am. Chem. Soc.* **1995**, *117*, 12793. (j) Brookhart, M.; Green, M. L. H. *J. Organomet. Chem.* **1983**, *250*, 395. (k) Yoshida, T.; Koga, N.; Morokuma, K. *Organometallics* **1995**, *14*, 746.

S0276-7333(97)00159-3 CCC: $15.00
Publication on Web 01/05/1998

Scheme 1

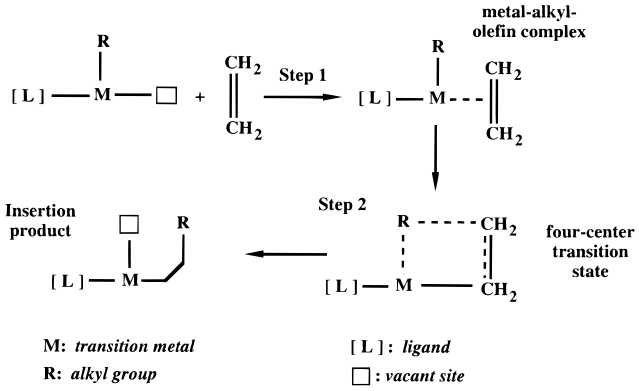

Scheme 2

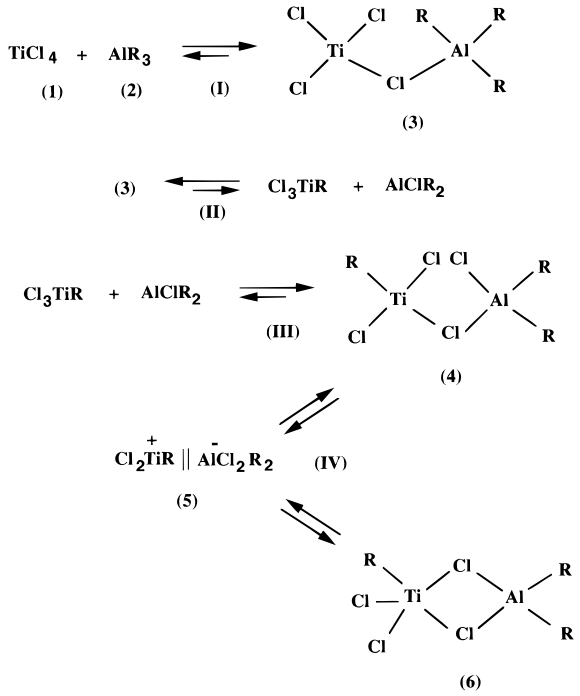

ecule. However many aspects of this mechanism are still obscure and need to be elucidated. In particular the existence of the intermediate metal−alkyl−olefin complex is still in doubt, and the nature of the active form of the catalyst has not been elucidated yet.

If we focus our attention on the commonly used two-component Ziegler−Natta catalyst $TiCl_4$−AlR_3, many experiments indicate that the active catalyst is formed in two subsequent equlibria (see Scheme 2) where the role of the Lewis acid AlR_3 is to promote by alkyl migration the formation of an unsaturated "cation-like" center. However the structural nature of the catalyst ($TiCl_4$)−cocatalyst (AlR_3) interaction is still obscure: the active species could be represented by a bimetallic complex as (4) or (6) or by a solvent separated ion pair as (5). The ion-pair hypothesis has recently been enforced by various experimental investigations.[2] In particular Eisch and co-workers[2e,d] have found that the rate of polymerization increases with the increasing polarity of the solvent which should favor the formation of the cation-like species through the equilibrium (IV).

In the past two decades many theoretical studies were carried out on this problem.[3] The majority of the computations used a cation-like fragment of the type $X_2TiCH_3^+$ as a model system for the active catalyst, while only a few computations were performed on a more complex model represented by a bimetallic species such as (4) or (6). A bimetallic system $(CH_3)_2Al(\mu\text{-}Cl)_2TiCl_2CH_3$, originated by the two fragments $TiCl_4$ and $Al(CH_3)_3$, was studied by Novaro et al.[3a] by means of the Hartree−Fock method. These authors, without optimizing the geometries of reactants and transition states, determined for ethylene insertion an activation energy of 15 kcal/mol, which is slightly overestimated with respect to the experimental value which varies in the range 5−12 kcal mol^{-1}.[1d,f,o] An activation energy of 4.3 kcal mol^{-1} was obtained by Kawamura[3c] who performed single-point MP2 computations on the Hartree−Fock-optimized geometries and pointed out the importance of the dynamical correlation energy.

More recently several studies were carried out where the effects of the dynamic correlation energy were included using different methods. These studies provided conflicting computational evidence concerning the existence of the transition state and that of a preliminary π-complex between the olefin and the catalyst. Meier, who performed ab initio (DFT) molecular dynamics simulations on the cationic model H_2SiCp_2-$ZrCH_3^+$(Cp = cyclopentadienyl),[3e] did not find any significant barrier for ethylene insertion. Similar evidence was obtained by Woo et al.[3f] who used the DFT method to study the cationic model $Cp_2ZrCH_3^+$. Weiss[3g] carried out MP2 and local spin density computations on the two-model systems $Cp_2ZrCH_3^+$ and $Cl_2TiCH_3^+$ and found that in the former case the reaction proceeds without barrier, while in the latter case there is an activation energy of 2.5 kcal mol^{-1}. Very recently a bimetallic model was reconsidered by Jensen et al.[3h] who tried to investigate the role of the cocatalyst in the homogeneous Ziegler−Natta process. These authors carried out Hartree−Fock computations on the model system formed by the bimetallic compund $H_2Al(\mu\text{-}Cl)_2TiCl_2CH_3$ and one ethylene molecule; to obtain a better energetics, they performed correlated calculations on the Hartree−Fock geometries using the modified coupled-pair function (MCPF) method. At this level these authors found that the potential energy surface is almost flat in the region between reactants and the point corresponding to the insertion transition state. Beyond this point the energy decreases to reach the products so that the reaction occurs without energy barrier.

In the present paper we discuss the results obtained for the bimetallic complex which forms from the two species $TiCl_4$ and $Al(CH_3)_3$. Our model is represented by the bimetallic species $H_2Al(\mu\text{-}Cl)_2TiCl_2CH_3$, where we have replaced the two methyl groups bonded to aluminum with two hydrogen atoms. To study this system we have used the density functional theory (DFT)[4,5] method with nonlocal corrections. Our aim is to obtain

(4) Parr, R. G.; Yang, W. *Density-Functional Theory of Atoms and Molecules*; Oxford University Press: New York, 1989.

(5) (a) Hohenberg, P.; Kohn, W. *Phys. Rev. B* **1964**, *136*, 864. (b) Kohn, W.; Sham, L. J. *Phys. Rev. A* **1965**, *140*, 1133. (c) Vosko, S. H.; Wilk, L.; Nusair, M. *Can. J. Phys.* **1980**, *58*, 1200. (d) Becke, A. D. *Phys. Rev.* **1988**, *A38*, 3098. (e) Lee, C.; Yang, W.; Parr, R. G. *Phys. Rev.* **1988**, *B37*, 785. (f) Miehlich, A.; Savin, A.; Stoll, H.; Preuss, H. *Chem. Phys. Lett.* **1989**, *157*, 200. (g) Becke, A. D. *J. Chem. Phys.* **1993**, *98*, 5648.

detailed information about the effect of the dynamic correlation energy on the structure of the insertion transition state and on the energy profile of the insertion step and the role played by the cocatalyst. For comparative purposes we have also re-examined the cationic model system $Cl_2TiCH_3^+$, which can be considered to emulate the positive fragment of a solvent-separated ion pair. In the latter case we have used different levels of theory (DFT, MP2, and CASPT2) to check the reliability of the computational approach used throughout the paper. For the cationic model we discuss in detail in the following section only the DFT results, and we report the data obtained with the other methods in the Appendix.

Computational Method

All DFT computations reported here were performed with the Gaussian 94[6] series of programs using the hybrid Becke's three-parameter exchange functional[5g] denoted here as B3LYP. Following the Gaussian 94 formalism this functional can be written in the following form:

$$0.80E(\mathrm{S})_x + 0.20E(\mathrm{HF})_x + 0.72E(\mathrm{B88})_x + 0.19E(\mathrm{LOCAL})_c + 0.81E(\mathrm{NON\text{-}LOCAL})_c$$

where $E(\mathrm{S})_x$ is the Slater exchange,[5a,b] $E(\mathrm{HF})_x$ the Hartree−Fock exchange, $E(\mathrm{B88})_x$ represents the Becke's 1988 nonlocal exchange functional corrections,[5d] $E(\mathrm{LOCAL})_c$ corresponds to the Vosko, Wilk, and Nusair local correlation functional,[5c] and $E(\mathrm{NON\text{-}LOCAL})_c$ to the correlation functional of Lee, Yang, and Parr ($E(\mathrm{LYP})_c$)[5e,f] which includes both local and nonlocal terms.

Two different basis sets were used. The simpler one corresponds to the MIDI4 basis set of Huzinaga[7] augmented by two sets of *p* functions on the titanium atom (exponent 0.083 and 0.028). The more accurate basis set was obtained using the 6-31G* basis[8] for carbon, aluminum, chlorine, and hydrogen and the Watchers−Hay basis[9] for titanium. The titanium basis is formed by a (14s,11p,6d) primitive set contracted to [8s,6p,4d]. This basis set will be simply denoted here as 6-31G*. In all cases the geometries of the various critical points were fully optimized with the gradient method. The nature of each critical point was characterized by computing the harmonic vibrational frequencies.

Results and Discussion

In this section we discuss in detail the singlet potential energy surface associated with the insertion of one ethylene molecule in the Ti−methyl bond for the cationic model $Cl_2TiCH_3^+$ and for the bimetallic species $H_2Al(\mu\text{-}Cl)_2TiCl_2CH_3$.

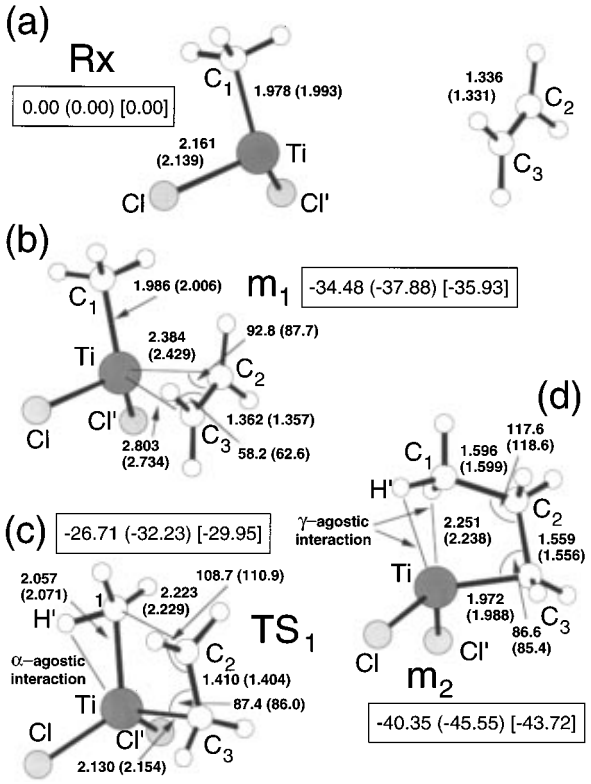

Figure 1. Schematic structures of (a) reactants Rx, (b) intermediate m_1, (c) transition state TS_1, and (d) product m_2 for the insertion reaction involving ethylene and $Cl_2TiCH_3^+$ (bond lengths are in angstroms and angles in degrees). The energy values are relative to reactants and have been obtained with the MIDI4 basis, the 6-31G* basis with geometry optimization (values in brackets), and the 6-31G* basis at the MIDI4-optimized geometries (values in square brackets). The absolute energies for reactants are: −1886.134 40 hartree (MIDI4), −1888.167 27 hartree (6-31G*) and −1888.169 69 hartree (6-31G* at the MIDI4-optimized geometries).

A. $(Cl_2TiCH_3)^+$ Model. In this case, in addition to the critical point corresponding to the reactants $Cl_2TiCH_3^+ + C_2H_4$ (Rx), we have located three additional critical points: a π-complex intermediate $Cl_2TiCH_3(C_2H_4)^+$ (m_1), a transition state (TS_1), and the insertion product $Cl_2Ti(C_3H_7)^+$ (m_2). The corresponding molecular structures are schematically represented in Figure 1 with the values of the most relevant geometrical parameters obtained with the two basis sets MIDI4 and 6-31G*. In the figure the energy values relative to reactants are also given. A more detailed tabulation of these geometries is reported in Table 1 of the Supporting Information.

The results obtained with the two basis sets do not differ significantly and are quite similar to those already discussed in previous papers.[3] In the following we discuss in detail only the 6-31G* data. The cationic fragment $Cl_2TiCH_3^+$ corresponding to the active catalyst (Figure 1a) is characterized by a pyramidal hybridization and by a C_s symmetry with the methyl group staggered with respect to the Ti−Cl bonds. The formation of the π complex m_1 between the $Cl_2TiCH_3^+$ moiety and the ethylene molecule leaves almost unchanged the

(6) Frisch, M. J.; Trucks, G. W.; Schlegel, H. B.; Gill, P. M. W.; Johnson, B. G.; Robb, M. A.; Cheeseman, J. R.; Keith, T.; Petersson, G. A.; Montgomery, J. A.; Raghavachari, K.; Al-Laham, M. A.; Zakrzewski, V. G.; Ortiz, J. V.; Foresman, J. B.; Peng, C. Y.; Ayala, P. Y.; Chen, W.; Wong, M. W.; Andres, J. L.; Replogle, E. S.; Gomperts, R.; Martin, R. L.; Fox, D. J.; Binkley, J. S.; Defrees, D. J.; Baker, J.; Stewart, J. P.; Head-Gordon, M.; Gonzalez, C.; Pople, J. A. Gaussian 94, Revision B.2 Gaussian, Inc., Pittsburgh, PA, 1995.

(7) (a) Takewaki, H.; Huzinaga, S. *J. Comput. Chem.* **1980**, *1*, 205. (b) Sakai, Y.; Takewaki, H.; Huzinaga, S. *J. Comput. Chem.* **1981**, *2*, 100. (c) Sakai, Y.; Takewaki, H.; Huzinaga, S. *J. Comput. Chem.* **1981**, *2*, 278.

(8) (a) Hariharan, P. C.; Pople J. A. *Theor. Chem. Acta* **1973**, *28*, 213. (b) Francl, M. C.; Petro, W. J.; Hehre, W. J.; Binkley, J. S.; Gordon, M. S.; Defrees, D. J.; Pople, J. A. *J. Chem. Phys.* **1982**, *77*, 3654.

(9) (a) Wachters, A. J. H. *J. Chem. Phys.* **1970**, *52*, 1033. (b) Wachters, A. J. H. *IBM Tech. Rep.* **1969**, RJ584. (c) Hay, P. J. *J. Chem. Phys.* **1977**, *66*, 4377.

Scheme 3

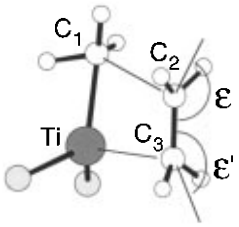

cationic fragment: only the Ti−C_1 bond and the ∠C_1-TiCl and ∠C_1TiCl′ angles slightly increase (from 1.993 to 2.006 Å and from 104.7° to 106.6° or 106.7°, respectively). The olefin bond and the Ti−CH_3 bond are not coplanar, and consequently, m_1 has a C_1 symmetry. The orientation of the ethylene molecule with respect to the Ti−methyl bond is described by the dihedral angle ω (64.6°) between the two planes C_2C_3Ti and C_1TiC_3 (this angle is denoted as $\omega[C_2(C_3Ti)C_1]$). In this complex the distances between the olefinic carbons and the metal atom are significantly different, the shorter (Ti−C_2) and the longer (Ti−C_3) distance being 2.429 and 2.734 Å respectively. As a consequence of the formation of the new Ti−C bonds, the olefin bond C_2−C_3 increases from 1.331 to 1.357 Å and a slight rehybridization of the two carbon atoms takes place. A mesasure of the pyramidalization of C_2 and C_3 is given by the two angles ϵ and ϵ' which are both defined in Scheme 3: ϵ corresponds to the angle between the C_2−C_3 bond and the HC_2H plane and ϵ' to the angle between the C_2−C_3 bond and the HC_3H plane (the value of these angles is 180° in the planar ethylene). ϵ and ϵ' are 167.2° and 178.2°, respectively, showing that the methylenic hydrogens bonded to C_2 and C_3 are slightly bent out of the ethylene molecular plane. A structure where the olefin bond and the Ti−CH_3 bond are coplanar ($\omega[C_2(C_3Ti)C_1] = 0$) has also been located. However this structure (not reported in Figure 1) is a conformational transition state connecting two equivalent m_1 complexes with a very low barrier.

TS_1 is a four-centered structure corresponding to the transition state for the ethylene insertion. The vibrational analysis shows that the normal mode with imaginary frequency is a linear combination of the two forming, C_1−C_2 and Ti−C_3, bonds and of the breaking, Ti−C_1, bond. Also here the ethylene double bond and the Ti−CH_3 bond are not coplanar even if the ω angle is very small (only 7.6°). The interaction between the metal and the ethylene molecule is now stronger (C_1−C_2 and Ti−C_3 are much shorter than in m_1 being 2.229 and 2.154 Å, respectively) and, consequently, the olefin bond has become longer (1.404 Å) since it is loosing its double bond character. This transition state is relatively early since the Ti−methyl bond, which is the bond being broken, is only 3.1% longer than in the π-complex. TS_1 is also characterized by a long C_1−H′ distance (1.138 Å) in the methyl group (see Figure 1c). This anomalous value found for C_1−H′ indicates a stabilizing α-agostic interaction which has been suggested to assist olefin insertion during the polymerzation process.[3c,g] A similar value for the distance of a C−H bond involved in agostic interactions has already been found by Morokuma et al. at the HF level.[3c]

The insertion product m_2 (propyl complex) is an approximately planar four-centered structure (ω is only 1.1°) where the two new C_2−C_1 and Ti−C_3 bonds are almost complete (1.599 and 1.988 Å, respectively). Also in this structure we can envisage two γ-agostic interactions as indicated by the long C−H′ distances (1.115 Å) in the methyl group.

The 6-31G* energy values reported in Figure 1 (values in brackets) show that the π-complex intermediate, which forms without any barrier, is 37.88 kcal mol^{-1} lower than the two reactant fragments. The barrier for ethylene insertion (computed with respect to m_1) is 5.65 kcal mol^{-1}, in good agreement with the experimental estimate of 5−12 kcal mol^{-1}.[1d,f,o] The insertion reaction is exothermic since the product propyl complex is 7.67 kcal mol^{-1} lower in energy than the intermediate m_1 and 45.55 kcal mol^{-1} lower in energy than reactants. These results indicate that the insertion reaction is indeed a very easy process.

A comparison of the results obtained at the two levels of accuracy MIDI4 and 6-31G* shows that these energies are not very sensitive to the basis set: at the MIDI4 level the reaction is slightly less exothermic (−40.35 kcal mol^{-1}) and the insertion barrier increases from 5.65 to 7.67 kcal mol^{-1}. It is very interesting to point out that the energy values obtained with the 6-31G* basis set at the MIDI4-optimized geometries (values in square brackets) are very close to the values obtained at the 6-31G*-optimized geometries: the insertion barrier is 5.98 kcal mol^{-1} and the reaction is exothermic by 43.72 kcal mol^{-1}. This computational evidence suggests that it is possible to obtain reliable energetics by performing single-point computations with an extended basis set on the geometries optimized at a lower level of accuracy. This strategy is particularly interesting for large systems, and we have adopted it (i.e. single-point 6-31G* computations on the MIDI4-optimized geometries) to study the potential surface for the bimetallic complex discussed in the following subsection.

B. $H_2Al(\mu\text{-}Cl)_2TiCl_2CH_3$ Model. On the potential surface corresponding to the reaction between the bimetallic complex and an ethylene molecule, we have located eight critical points schematically represented in Figures 2−4: the reactants (Rx), a transition state for the formation of an ethylene π complex (TS_2), the π-complex (m_3), three transition states for ethylene insertion (TS_3, TS_4, and TS_5), and two product propyl complexes (m_4 and m_5). In these figures we have reported the optimum values of the most relevant geometrical parameters and the energy values relative to reactants. A detailed tabulation of the various geometrical parameters for these structures is reported in Table 2 of the Supporting Information.

In the complex corresponding to reactants (Figure 2a) the metal atom is characterized by a distorted trigonal−bipyramidal configuration where the methyl group and the two chlorine atoms Cl_1 and Cl_3 are approximately in equatorial positions while Cl_2 and Cl_4 are axial. The nonequivalence of the three equatorial substituents and the constraint of the bridging bonds are responsible for the distortion of this structure with respect to a regular bipyramid. A significant lengthening of the Ti−Cl bonds characterizes the bridged ring system: the Ti−Cl_3 and the Ti−Cl_4 bonds are 2.517 and 2.568 Å, respectively, while Ti−Cl_1 and Ti−Cl_2 are 2.218 and 2.236 Å. Placing the methyl group and the Cl_3 chlorine

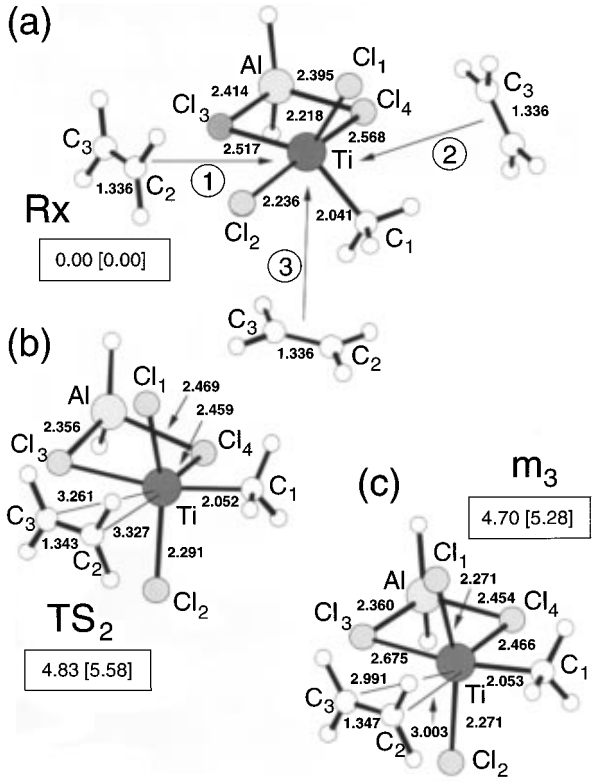

Figure 2. Schematic structures of (a) reactants Rx, (b) transition state TS_2 leading to the π complex, and (c) π complex m_3 for the insertion reaction involving ethylene and the bimetallic species $H_2Al(Cl_2)TiCl_2CH_3$ (bond lengths are in angstroms and angles in degrees). The energy values are relative to reactants and have been obtained with the MIDI4 basis and the 6-31G* basis at the MIDI4-optimized geometries (values in square brackets). The absolute energies for reactants are −3049.348 14 hartree (MIDI4) and −3052.645 21 hartree (6-31G* at the MIDI4-optimized geometries).

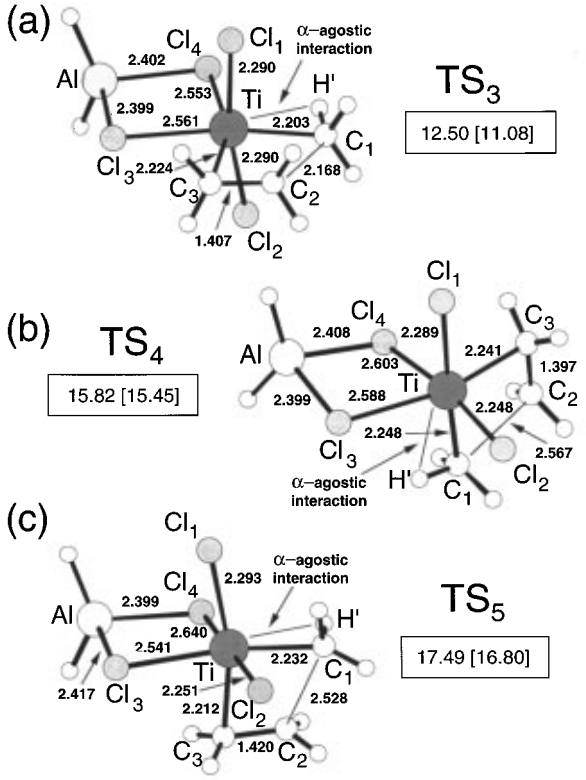

Figure 3. Schematic structures of the three insertion transition states TS_3 (a), TS_4 (b), and TS_5 (c) for the insertion reaction involving ethylene and the bimetallic species $H_2Al(Cl_2)TiCl_2CH_3$ (bond lengths are in angstroms and angles in degrees). The energy values are relative to reactants and have been obtained with the MIDI4 basis and the 6-31G* basis at the MIDI4-optimized geometries (values in square brackets).

atom in axial positions leads to a structure of C_s symmetry which is slightly higher in energy (only 0.7 kcal mol^{-1}). In this structure the titanium and aluminum atoms, the two chlorine atoms Cl_3 and Cl_4, and the methyl group lie on the symmetry plane and the two bonds $Ti-Cl_1$ and $Ti-Cl_2$ are equivalent (2.219 Å). This structure, which is not reported in Figure 2, is a transition state connecting two equivalent Rx structures as demonstrated by the frequency computation. We have also investigated the existence of a bimetallic complex with only one chlorine atom in a bridging position (4 in Scheme 2), but in spite of extensive search, no critical point of this type has been located on the surface.

In exploring the insertion process in the titanium−methyl bond we have considered the approach of the ethylene molecule along three different directions which are schematically represented in Figure 2a. The approach occurring along direction 1 leads to the formation of a weak π complex (m_3 in Figure 2c) characterized by a C_s symmetry. The weak complexation is proved by the C_2-C_3 distance in the ethylene fragment which is only slightly larger (1.347 Å) than in free ethylene (1.336 Å) and by the long carbon−titanium bonds $Ti-C_3$ and $Ti-C_2$ which are 2.991 and 3.003 Å respectively. However, even if the interaction is weak, it is responsible for a rotation of the chlorine atoms Cl_1 and Cl_2 and of the methyl group around the Ti−Al axis and for the appearance of a plane of symmetry ($TiCl_3Cl_4Al$ plane). After rotation the methyl group moves from a pseudoequatorial position to a pseudoaxial position, and the two $Ti-Cl_1$ and $Ti-Cl_2$ bonds become equivalent (2.271 Å). Along the reaction path leading to m_3 we have located a transition state (TS_2 in Figure 2b), as demonstrated by the frequency computation that shows an imaginary mode dominated by the motion of the ethylene molecule toward the complex. The structure of TS_2 is very similar to that of the π complex even if the C_s symmetry is only approximate as shown by the two $Ti-Cl_1$ and $Ti-Cl_2$ bonds which are slightly different (2.280 and 2.291 Å, respectively). If we move further along direction 1 beyond the π complex, the energy rises to reach a transition state corresponding to the insertion of the ethylene molecule in the Ti−methyl bond (TS_3 in Figure 3a). In this structure, which maintains the C_s symmetry and is similar to that already described by Jensen et al.,[4h] the titanium has approximately reached an octahedral configuration with the two chlorine atoms in axial positions. The new forming $Ti-C_3$ bond is 2.224 Å, while the olefin bond, as a consequence of the larger interaction, has become 1.407 Å. A significant rehybridization of the C_2 and C_3 atoms also occurs as already pointed out in the previous section for the cationic model (the two angles ϵ and ϵ' are 153.0° and 154.3°, respectively). The breaking bond $Ti-C_1$ and the new forming bond C_1-C_2 are respectively longer (2.203 Å) and shorter (2.168 Å) than the corresponding bonds in the

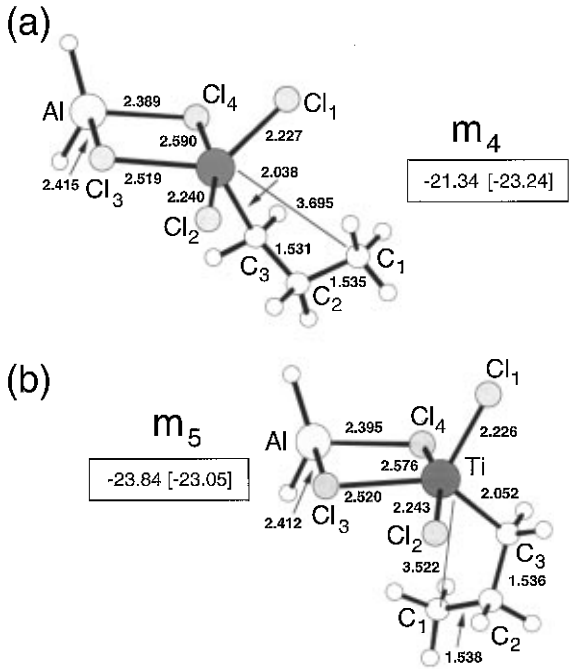

Figure 4. Schematic structures of the two propyl products m_4 (a) and m_5 (b) for the insertion reaction involving ethylene and the bimetallic species $H_2Al(Cl_2)TiCl_2CH_3$ (bond lengths are in angstroms and angles in degrees). The energy values are relative to reactants and have been obtained with the MIDI4 basis and the 6-31G* basis at the MIDI4-optimized geometries (values in square brackets).

transition state located for the cationic model. Thus this transition structure seems to have more product-like character than the analogous structure found for the charged system. Also in this transition state the α-agostic interaction involving the in-plane methyl hydrogen H′ and the metal atom is quite evident as indicated by a C_1-H' bond length of 1.122 Å and a Ti−H′ distance of 2.098 Å.

Two additional transition states for ethylene insertion have been located along directions 2 (TS_4) and 3 (TS_5). These two transition states are of C_1 symmetry but the arrangement of the atoms involved in the insertion process is similar to that previously described for TS_3 with the methyl, the two olefin carbon atoms and the titanium atom approximately coplanar in both cases ($\omega[C_2(C_3Ti)C_1]$ is 3.4° and 6.7° in TS_3 and TS_4, respectively). The most significant differences in comparing TS_3 with TS_4 and TS_5 are found in the length of the new forming bond C_1-C_2 and the breaking bond Ti−C_1: C_1-C_2 is 2.567 and 2.528 Å in TS_4 and TS_5, respectively, while the corresponding values of Ti−C_1 are 2.248 and 2.232 Å. As a consequence of the longer Ti−C_1 distances the α-agostic interaction involving a methyl hydrogen and the titanium atom becomes weaker as indicated by the shorter C_1-H' bond (1.112 and 1.108 Å in TS_4 and TS_5, respectively) and the longer Ti-H′ distance (2.156 and 2.242 Å respectively).

On the product side of the potential surface we have located two critical points (m_4 and m_5, Figure 4) corresponding to different conformations of the propyl complex. In both complexes the configuration of the titanium atom is identical to that already described for reactants, i.e. a distorted trigonal-bipyramidal configuration where the propyl group, Cl_1 and Cl_3 are approximately in equatorial positions and Cl_2 and Cl_4 are axial. In the two complexes the agostic interactions have become negligible, the Ti−H′ distances being in both cases greater than 2.4 Å.

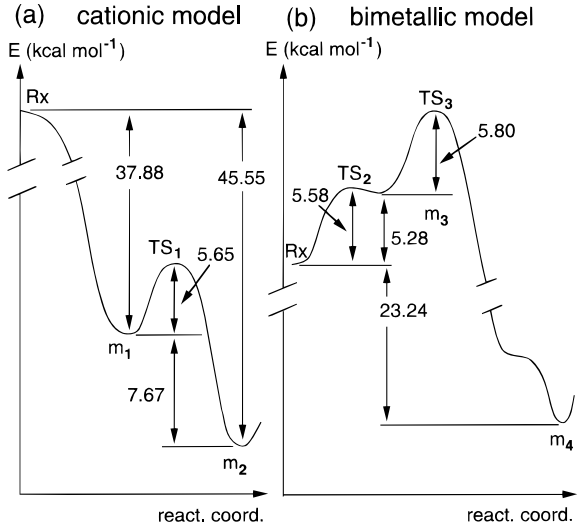

Figure 5. Energy profiles for the insertion reaction involving (a) the cationic species $Cl_2TiCH_3^+$ and (b) the bimetallic species $H_2Al(Cl_2)TiCl_2CH_3$.

We discuss now the energetics of the reaction, and we use to this purpose the energy values obtained with the more extended basis set 6-31G* (values in square brackets). The results previously discussed indicate that three different reaction channels exist on the reaction surface leading to the final propyl complexes. Only one (channel 1) of the three reaction pathways involve the formation of a preliminary π complex, which is 5.28 kcal mol^{-1} higher than reactants. To form this complex a barrier of 5.58 kcal mol^{-1} must be overcome. From the π complex it is possible to reach the product region through the transition state TS_3 and an additional barrier of 5.80 kcal mol^{-1}. Thus this energy profile differs significantly from that found for the cationic species where the π-complex forms without any barrier: these two energy profiles (cationic model and bimetallic model) are compared in Figure 5. The two remaining channels (2 and 3) associated with the bimetallic species lead directly to the formation of the insertion product through the two transition states TS_4 and TS_5. These pathways are energetically less favorable since the corresponding activation barriers are 15.45 and 16.80 kcal mol^{-1}, respectively. The energy values of the insertion products show that the reaction is exothermic and that the two different conformations, m_4 and m_5, of the propyl complex are almost degenerate. It is interesting to point out that these two forms of the propyl complex do not correlate directly with channel 1 but with channels 2 and 3. As a resulting product of channel 1, one would expect a propyl complex of C_s symmetry with the propyl fragment on the same plane of the bridged ring. However a stable structure of this type has not been located.

To obtain more detailed information about channel 1, we have computed the reaction pathway starting from

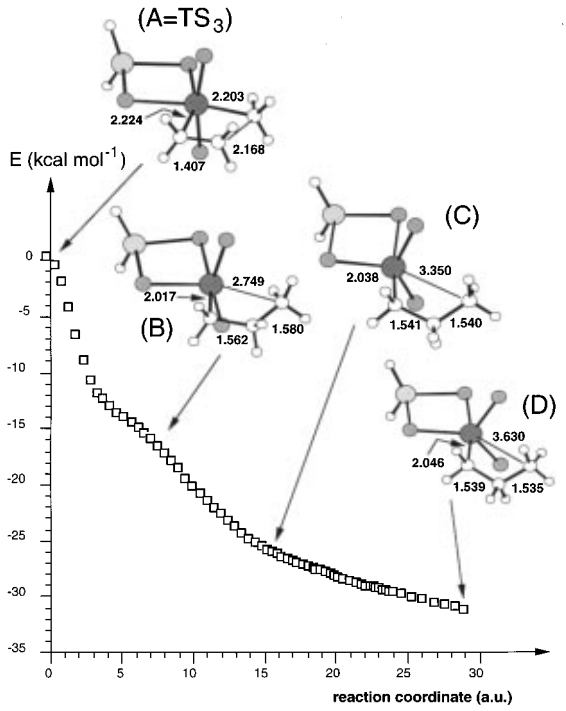

Figure 6. Energy as a function of the path coordinate connecting TS_3 to the propyl product region.

the transition state TS_3 in the product direction (IRC).[10] To this purpose we have used the Gonzales and Schlegel method[10b,c] as implemented in Gaussian 94. The computed potential energy curve and the changes of the most important geometrical parameters along the reaction path are presented in Figure 6. The starting point of the energy profile is the transition state TS_3 (structure A) where the two atoms C_2 and C_1 are still quite far away (2.168 Å) and the breaking bond $Ti-C_1$ is only slightly longer (2.203 Å) than the standard value (about 2.05 Å). The two intermediate structures B and C correspond to a further increase of the $Ti-C_1$ distance (2.749 and 3.350 Å, respectively) and a decrease of the C_1-C_2 distance which becomes 1.580 and 1.540 Å, respectively. This reaction path, which includes 60 points on the potential energy surface, leads to a very flat region corresponding to a propyl complex of C_s symmetry (structure D). However this structure does not corresponds to a real minimum of the surface since, after geometry optimization, it collapses to the m_4 complex 4.25 kcal mol^{-1} lower in energy.

All these results are significantly different from those obtained by Jensen et al.[3h] These authors, who did not include the correlation effect in the geometry optimization but carried out MCPF computations on the Hartree−Fock optimized geometries, found that the reaction occurs without any barrier and concluded that the dissociation of the catalyst into a solvent-separated ion pair $(CH_3)_2AlCl_2^- \,||\, Cl_2TiCH_3^+$ is not necessary to make the insertion reaction possible. On the contrary our computations show that, even if the reaction involving the bimetallic species as active catalyst is possible, a significant barrier must be overcome along all three different channels available on the potential surface.

Conclusion

In this paper we have studied the potential energy surface for the insertion reaction of ethylene in the titanium−carbon bond which represents a fundamental step in Ziegler−Natta polymerization reactions. Since one of the purposes of this study was to establish if the active catalyst exists as a solvent separated ion pair or bimetallic complex, we have considered two different models: (1) the cationic species $Cl_2TiCH_3^+$ reacting with an ethylene molecule and (2) the bimetallic species $H_2Al(Cl_2)TiCl_2CH_3$ reacting with ethylene. In the first case we have tried to emulate the positive part of a solvent separated ion pair $(CH_3)_2AlCl_2^- \,||\, Cl_2TiCH_3^+$ which is supposed to form when a mixture of $(CH_3)_3Al$ and $TiCl_4$ is used as Ziegler−Natta catalyst. In the latter case we have tried to mimic the possible bimetallic complexes or tight ion pairs which can originate from the catalyst−cocatalyst interaction (see Scheme 2). To investigate the potential surface, we have used a DFT approach based on the three-parameters Becke functional. The reliability of this approach has been accurately checked by comparing its results with those obtained at the MP2 and CASPT2 levels (see Appendix).

We have found that for both model systems one or more reaction pathways exist which lead to the final insertion product, suggesting that both species can behave in principle as active catalysts. However the reaction profiles obtained in the two cases are quite different. In the first case we have observed the formation of a π-complex intermediate, much lower in energy than reactants (37.88 kcal mol^{-1}), and the process does not require any barrier. From the intermediate the insertion proceeds with a barrier of 5.65 kcal mol^{-1} leading to the final propyl complex 7.67 kcal mol^{-1} lower in energy than the intermediate and 45.55 kcal mol^{-1} lower in energy than reactants.

In the second case we have demonstrated the existence of three reaction channels leading to the insertion product. The energetically most favored channel is a two-step reaction path since it involves the formation of an intermediate π-complex. This path requires the overcoming of a first barrier of 5.58 kcal mol^{-1} to form the intermediate (which corresponds to a very shallow minimum of the surface 5.28 kcal mol^{-1} higher in energy than reactants) and of a second barrier of 5.80 kcal mol^{-1} to reach the TS_3 insertion transition state.

These results seem to indicate that the reaction can proceed more easily in the case of a separated ion pair where only one energy barrier of about 5.6 kcal mol^{-1} must be overcome and the exothermicity is higher. However an important point must be discussed to better understand the meaning of the computations carried out on the two models. Ab initio computations provide results which can be thought to emulate real molecules in gas phase. In such a situation a bimetallic complex as that considered in this paper is thermodynamically

(10) (a) Fukui, K. *Acc. Chem. Res.* **1981**, *14*, 363. (b) Gonzales, C.; Schlegel, H. B. *J. Phys. Chem.* **1990**, *94*, 5523. (c) Gonzales, C.; Schlegel, H. B. *J. Chem. Phys.* **1991**, *95*, 5853.

(11) (a) Miertus, S.; Scrocco, E.; Tomasi, J. *Chem. Phys.* **1981**, *65*, 239.(b) Miertus, S.; Tomasi, J. *Chem. Phys.* **1982**, *65*, 239. (c) Keith, T. A.; Frisch, M. J., manuscript in preparation.

(12) Andersson, K.; Malmqvist, P.; Roos, B. O.; Sadlej, A. J.; Wolinski, K. *J. Phys. Chem.* **1990**, *94*, 5483. Andersson, K.; Malmqvist, P.; Roos, B. O. *J. Chem. Phys.* **1992**, *96*, 1218.

(13) MOLCAS version 3, Andersso, K.; Fulscher, M. P.; Lindth, R.; Malmqvist, P.; Olsen, J.; Roos, B. O.; Sadlej, A. J. University of Lund, Sweden, and P.O. Widmark, IBM, Sweden, 1991.

Table 1. Insertion Energy Barriers (ΔE)[a,b] Computed for the Cationic Model and the Bimetallic Model in Different Environments (Dielectric Constant ϵ) Using the SCI-PCM Method and the 6-31G* Basis Sets

	ΔE	
environment (ϵ)	cationic model	bimetallic model
gas-phase	5.63	5.80
2.38	4.46	4.69
4.33	3.03	4.14
9.08	2.61	3.63

[a] ΔE corresponds to the energy difference between the intermediate π-complex and the insertion transition state. For the cationic model the absolute energy for the intermediate is −1888.276 78 (ϵ = 2.38); −1888.292 12 (ϵ = 4.33); −1888.302 95 (ϵ = 9.08). For the bimetallic model the absolute energy for the intermediate is −3052.639 51 (ϵ = 2.38); −3052.640 90 (ϵ = 4.33); −3052.636 06 (ϵ = 9.08). [b] Energy values are in kcal mol^{-1}.

much more stable than the two noninteracting ions $(CH_3)_2AlCl_2^-$ and $Cl_2TiCH_3^+$. As a consequence, in a hypothetical gas phase the reaction pathway involving the cationic species seems to be too high in energy to be easily available (equilibrium IV in Scheme 2 is shifted to the right) and the reaction can be thought to proceed mainly through the formation of a bimetallic complex.

A polar solvent can stabilize the ion pair and can shift significantly equilbrium IV to the left. This stabilization would have the effect of lowering the energy of the reaction channel associated with the cationic species (which would become more easily available) and that of increasing the overall reaction rate since for the cation only one reaction barrier of 5.65 kcal mol^{-1} must be overcome. To roughly evaluate how much the solvent affects the energy of the ion pair and the insertion barrier, we have carried out self-consistent reaction field (SCRF) computations on both cationic and bimetallic models. In particular we have used the self-consistent isodensity polarized continuum model (SCI-PCM)[11] available in Gaussian 94 and we have emulated three different solvents: (i) toluene (dielectric constant ϵ = 2.38), (ii) diethyl ether (ϵ = 4.33), (iii) dichloromethylene (ϵ = 9.08). For each environment, corresponding to a different values of ϵ, we have evaluated the insertion energy barrier corresponding to the energy difference between the intermediate π-complex and the insertion transition state. For the bimetallic model we have considered the lowest energy transition state TS_3. In all cases we have kept the geometries frozen at the values obtained in the gas phase (Figures 1−4). The results obtained from these computations on the two models are collected in Table 1 and show that the energy barriers decrease with the increasing polarity of the solvent. Furthermore in a polar solvent the insertion energy barrier for the cationic species becomes smaller than that associated with a bimetallic complex.

Within this mechanistic scenario both reaction channels (bimetallic complex and separated ion pair) would be simultaneously available in the real conditions used to carry out the reactions. The relative importance of the two reaction pathways and the resulting reaction rate would depend mainly on the solvent polarity: the more polar the solvent, the more important the reaction path involving the cationic species. In such a situation two effects should contribute to increase the overall reaction rate in a polar solvent: (i) the decrease of the insertion energy barrier and above all (ii) the increasing importance of the reaction path involving the cationic species which is more exothermic and characterized by a lowest energy barrier. This hypothesis could explain some recent results[2d,e] which demonstrate that the reaction rate increases significantly with the increasing polarity of the solvent.

Appendix: MP2 and CASPT2 Computations on $(Cl_2TiCH_3)^+$

To validate the DFT approach we have computed the potential energy surface for the reaction between the cationic species $Cl_2TiCH_3^+$ and ethylene at the MP2 and CASSCF/CASPT2[12] levels of theory using the MIDI4 basis set. For the MP2 calculations we have used the Gaussian 94 series of programs, while the CASPT2 computations have been carried out with the MOLCAS-2 software.[13] The values of the geometrical parameters optimized at the MP2 and CASSCF levels and the corresponding energy values are reported in Table

Table 2. Energy Values Relative to Reactants (E, E^{PT2})[a,b] and Optimum Values[c] of the Most Relevant Geometrical Parameters for the Various Critical Points Located at the MP2 and CASSCF Levels with the MIDI4 Basis Set for the Reaction between $Cl_2TiCH_3^+$ and C_2H_4

	Rx		m_1		TS_1		m_2	
	MP2	CAS	MP2	CAS	MP2	CAS	MP2	CAS
C_2-C_3	1.354	1.343	1.376	1.360	1.422	1.412	1.588	1.531
$Ti-C_1$	2.020	2.229	2.031	2.204	2.073	2.204	2.271	2.475
Ti−Cl	2.169	2.207	2.185	2.226	2.198	2.235	2.206	2.242
Ti−Cl′	2.169	2.207	2.183	2.226	2.191	2.236	2.206	2.223
$Ti-C_3$	∞	∞	2.678	2.849	2.197	2.239	2.009	2.151
$Ti-C_2$	∞	∞	2.632	2.521	2.224	2.177	1.615	1.563
$\angle TiC_3C_2$			73.1	62.2	85.7	86.3	84.8	91.8
$\angle TiC_2C_3$			76.8	89.2	110.6	114.8	119.1	116.3
$\angle C_1TiCl$	103.6	101.4	107.1	101.9	114.5	111.8	120.2	118.4
$\angle C_1TiCl'$	103.6	101.5	106.1	101.6	115.8	111.6	119.7	122.4
ω[d]			104.2	144.1	9.0	1.7	2.3	11.0
ϵ	180.0	180.0	173.0	164.2	157.2	150.9	118.6	118.3
ϵ'	180.0	180.0	174.8	177.0	151.3	155.7	129.5	141.8
E	0.00	0.00	−34.47	−32.25	−25.74	−17.71	−39.44	−27.30
E^{PT2}		0.00		−35.15		−28.62		−37.25

[a] E^{PT2} represents the CASPT2 energy at the CASSCF-optimized geometries. The absolute energy for reactants is −1883.195 91 hartree at the MP2 level, −1882.786 27 hartree at the CASSCF level, and 1883.333 09 hartree at the CASPT2 level. [b] Energy values are in kcal mol^{-1}. [c] Bond lengths are in angstroms and angles in degrees. [d] ω is defined as $\omega = \omega[C_2(C_3Ti)C_1]$.

2. The CASPT2 energy values have been obtained by means of single-point CASPT2 computations on the CASSCF-optimized geometries. The active space used in the CASSCF computations includes the ethylene π and π^* orbitals, the σ and σ^* orbitals associated with the Ti−C_1 bond, and the empty $3d_z^2$, $3d_{xy}$, and $3d_{yz}$ orbitals on the metal atom.

Inspection of Table 2 shows that for the insertion transition state (TS_1) and the propyl product (m_2) the results obtained at the MP2 and DFT levels (MIDI4 basis set) are very similar. Also at the MP2 level both structures are characterized by a stabilizing agostic interaction involving the methyl hydrogen (H′ in Figure 1c,d) and the titanium atom. More significant differences, mainly associated with the Ti−C_2 and Ti−C_3 distances and the $\angle C_2C_3Ti$ and $\angle C_3C_2Ti$ angles, have been found in the intermediate π complex m_1. While at the DFT level, in the m_1 structure, the distance Ti−C_3 (2.803 Å) is significantly longer than Ti−C_2 (2.384 Å), and consequently the angle $\angle C_3C_2Ti$ (92.8°) is considerably larger than $\angle C_2C_3Ti$ (58.2°) at the MP2 level Ti−C_2 and Ti−C_3 and the corresponding angles $\angle C_2C_3Ti$ and $\angle C_3C_2Ti$ have very similar values (2.678 and 2.632 Å and 73.1° and 76.8°, respectively). Since in this structure the ethylene−catalyst interactions are very weak, the differences found at the two computational levels can be ascribed to a very flat surface which induces significant changes of the relative positions of the two fragments without affecting significantly the energy of the system.

Also the energetics of the reaction determined at the MP2 level is very similar to that discussed in the previous section at the DFT level. The reaction is exothermic by 39.44 kcal mol^{-1}, and the insertion barrier is 8.73 kcal mol^{-1}. These values must be compared with the values of 40.35 and 7.77 kcal mol^{-1} determined at the DFT/MIDI4 level.

To verify the validity of a single reference approach to describe the insertion process, we have investigated the potential surface using the CASSCF method. The topology of the surface obtained at this level of theory is identical to that already described at the DFT and MP2 levels. This finding is in agreement with the fact that the CASSCF wave function is mostly dominated by the SCF configuration, the coefficients for this configurations being in all cases larger that 0.95.

Even if the number and the nature of the various critical points do not change when a multireference wave function is used, for several geometrical parameters the difference between the values determined at the CASSCF level and the corresponding DFT values is more significant than the difference found between the MP2 values and the DFT values. The largest variations are observed in the forming and breaking bonds (Ti−C_1, Ti−C_3, and Ti−C_2 parameters) in the insertion transition state TS_1 and in the propyl product m_2. These differences are probably due to the fact that at the CASSCF level the largest part of the dynamic correlation energy is neglected. For this reason the energetics obtained at this level of theory are not expected to be reliable: inspection of Table 2 shows that the exothermicity of the reaction obtained with the CASSCF method decreases notably (−27.30 kcal mol^{-1}) while the barrier to insertion becomes much larger (14.54 kcal mol^{-1}). It is interesting to note that when the correlation energy is included by means of single-point CASPT2 computations on the CASSCF-optimized geometries, the energetic values become very similar to those determined at the MP2 and DFT levels: the reaction is now exothermic by 37.25 kcal mol^{-1} and the barrier is 6.53 kcal mol^{-1}. All of these results indicate that the DFT level of theory based on the three-parameter Becke functional and used throughout the work is adequate to describe this type of reactions and confirm the importance of the dynamical correlation to obtain a reliable description of both the geometry and energetics of these systems.

Supporting Information Available: Tables of geometrical parameters obtained with MIDI4 and 6-31G* (4 pages). Ordering information is given on any current masthead page.

OM970159T